American Mineralogist, Volume 77, pages 121–125, 1992

Stacking faults in synthetic celsian

L. S. Zevin
Institutes for Applied Research, Ben-Gurion University, P.O. Box 1025, Beer-Sheva, Israel

Abstract

Synthetic celsian (barium feldspar) crystallized from a glass of nearly stoichiometric composition exhibited a diffraction pattern with very broad and almost absent diffraction peaks with l = odd indices (the basic ≈7.2-Å cell is assumed). Three models based on the random shift of layers by **c**/2 are proposed to explain the phenomenon: (1) twinning by the Carlsbad law, (2) coesite-like distortion, and (3) faulting in the (100) plane. A comparison of observed and calculated peak widths showed that the third model was not applicable. The trend in the change in lattice parameters was most compatible with the first model, and observed diffraction effects thus appear to be caused by random twinning faults.

Introduction

In a study of the composition of synthetic glass-ceramics in the SiO_2-Al_2O_3-BaO-TiO_2 system we discovered an unusual diffraction effect related to feldspars. The major crystalline phase in this material is celsian (barium feldspar, $BaAl_2Si_2O_8$). Glass ceramics annealed in the temperature range 1000–1300 °C exhibit the diffraction pattern of celsian but with very broad or almost absent diffraction peaks with l = odd indices (indexing is based on a $c \approx 7.2$-Å cell, representing the basic structural unit) (Bogdanova et al., 1965). As the annealing temperature was allowed to rise, these diffraction peaks became sharper, and after annealing at 1350 °C the usual celsian pattern compatible with calculated data (Borg and Smith, 1969) was obtained. These diffraction effects might be expected from layered crystals faulted by a random shift of layers by half the c period. Despite the availability of an extensive body of literature on structural imperfections in feldspars (Smith, 1974), such diffraction effects have not been reported. It is possible that the phenomenon observed might be important in the elucidation of the crystallization behavior of feldspars. In this paper, three possible models for the observed faulting in celsian are proposed and compared with experimental diffraction data.

Experimental

Celsian was crystallized by mixing silica, alumina, and barium carbonate in proportions close to the stoichiometric composition of celsian. The mixture was doped with 3% TiO_2 as a nucleation aid. Melt was obtained at ~1800 °C, and glass was produced by cooling the melt in air. Annealing was then carried out for 2 h at temperatures ranging from 950 to 1350 °C.

Annealed samples were ground manually to pass a 325-mesh sieve, and diffraction patterns were obtained by conventional X-ray powder diffraction using Cu$K\alpha$ radiation (Fig. 1). The major crystalline phase was found to be celsian. The only minor phase detected was aluminum titanate Al_2TiO_5. The degree of crystallization estimated by X-ray diffraction reached 80% at 1300 °C (Bogdanova et al., 1965). Broadening and gradual loss of diffraction peaks with l odd indices is clearly visible in Figure 1.

Lattice parameters were obtained by least-squares refinement for samples crystallized at 1300 and 1100 °C. Twenty well-resolved diffraction peaks in the region $15° < 2\theta < 60°$ were used for the first sample, whereas only 12 reflections were available for the second sample. Lattice parameters are given in Table 1. The diffraction peak widths were measured at their half height. Instrumental broadening estimated by the full width at half maximum of a well-crystallized sample of α quartz was almost constant in the region $20° < 2\theta < 50°$ and equal to ~0.15°. This value was subtracted from the peak width of the samples investigated, and corrected values are given in Table 2.

Models for stacking faults

The following models for stacking faults were inspired by the view of the feldspar structure expressed by Belov (1953). The basic structural unit is, of course, a four-membered ring of Si,Al tetrahedra. These rings are connected in chains along the [100] and [001] directions (Fig. 2a). Two adjacent [001] chains have different elevations over the (010) mirror plane. The chain drawn in thick lines on Figure 2a is regarded as the upper one, whereas the adjacent chain (thin lines) is the lower one. Chains in the [100] direction exhibit the well-known crankshaft features, the thick-line and thin-line rings representing upper and lower horizontal (approximately) crankshaft parts, respectively. Ba cations (not shown in Fig. 2a) are situated in cavities between the [100] chains.

0003–004X/92/0102–0121$02.00

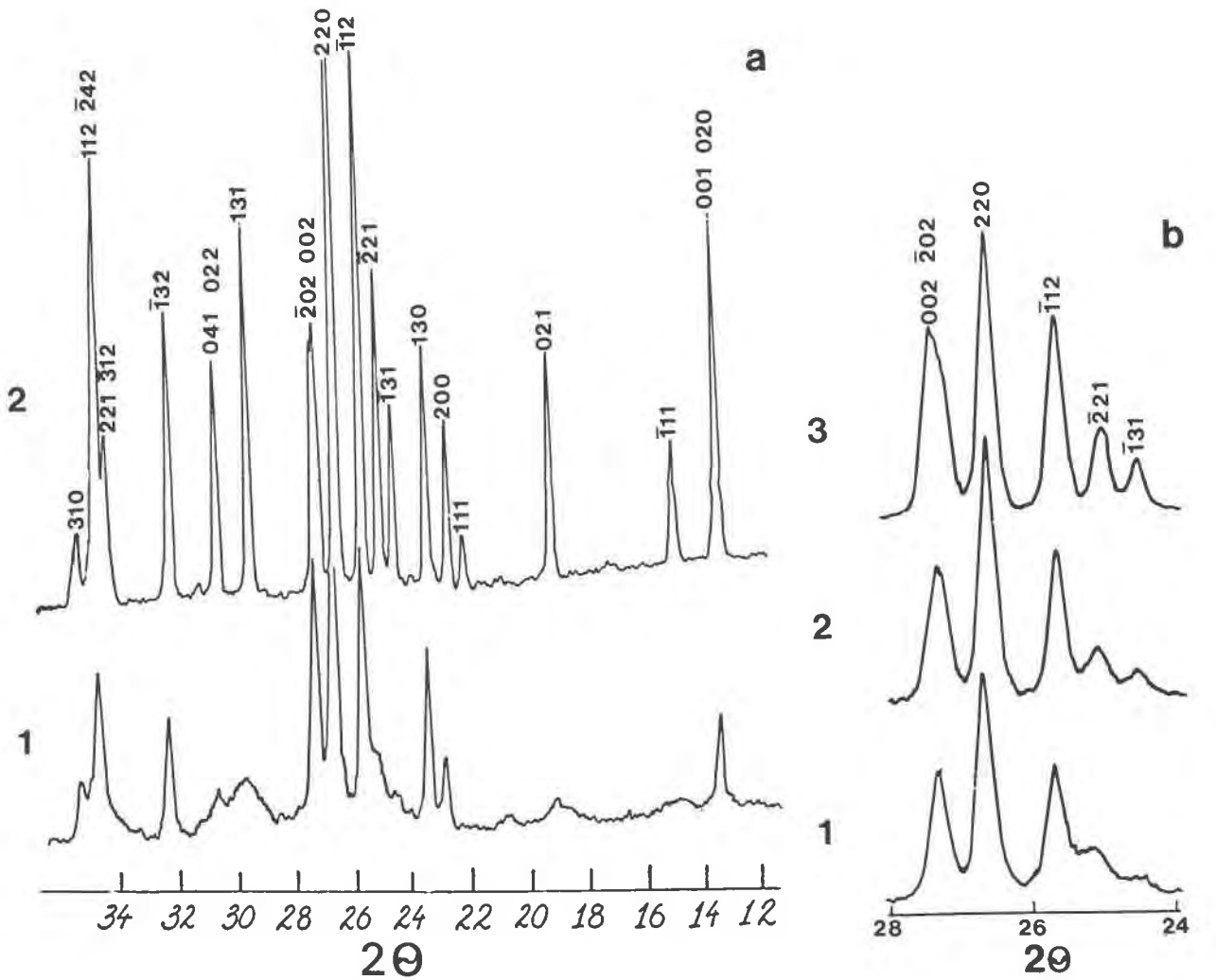

Fig. 1. Diffraction patterns of celsian glass ceramics obtained during the process of crystallization during annealing for 2 h: **(a)** 1, 2—annealing temperatures 1050, 1350 °C; **(b)** 1, 2, 3—annealing temperatures 1100, 1200, 1300 °C.

Each four-membered ring indicated by the thick lines in Figure 2a represents the lower portion of the real "thick" ring. Its upper portion (not shown in Fig. 2a) is a reflection of the lower portion in the (010) mirror plane. The nodes O1 are common to the lower and upper portions of the ring. The connection between the two halves of the same ring is clearly seen in Figure 3a, the view of the chain being in a direction normal to the (100) plane. The thin-line rings in Figure 2a have the same feature, of course, but only the upper portions are visible in Figure 2a. This is why thick-line and thin-line chains extended in the [001] directions look different: the figure shows the lower half of the former but the upper half of the latter. Now if we imagine the 001 face of the unit cell in Figure

Table 1. Lattice parameters of celsian

Crystallization temperature (°C)	*a* (Å)	*b* (Å)	*c* (Å)	*β* (°)
1100	8.586(9)	13.055(7)	7.203(5)	114.85(11)
1300	8.649(9)	13.066(9)	7.219(7)	115.22(11)

Table 2. Calculated and observed full width at half maximum of diffraction (FWHM) peaks with l = odd

hkl	Observed $\Delta 2\theta$ (°)*	Calculated $\Delta 2\theta$ (°) (010) faulting plane	Calculated $\Delta 2\theta$ (°) (100) faulting plane
021	0.90	0.71	0.51
131	0.75	0.73	1.13
041	0.70	0.93	0.33
113	0.30	0.20	0.19
151	1.10	1.00	0.35
331	0.35	0.53	1.55

Note: Observed values listed are the true FWHM corrected for the effects of instrumental peak broadening (0.15° 2θ).
* Sample annealed at 1050 °C.

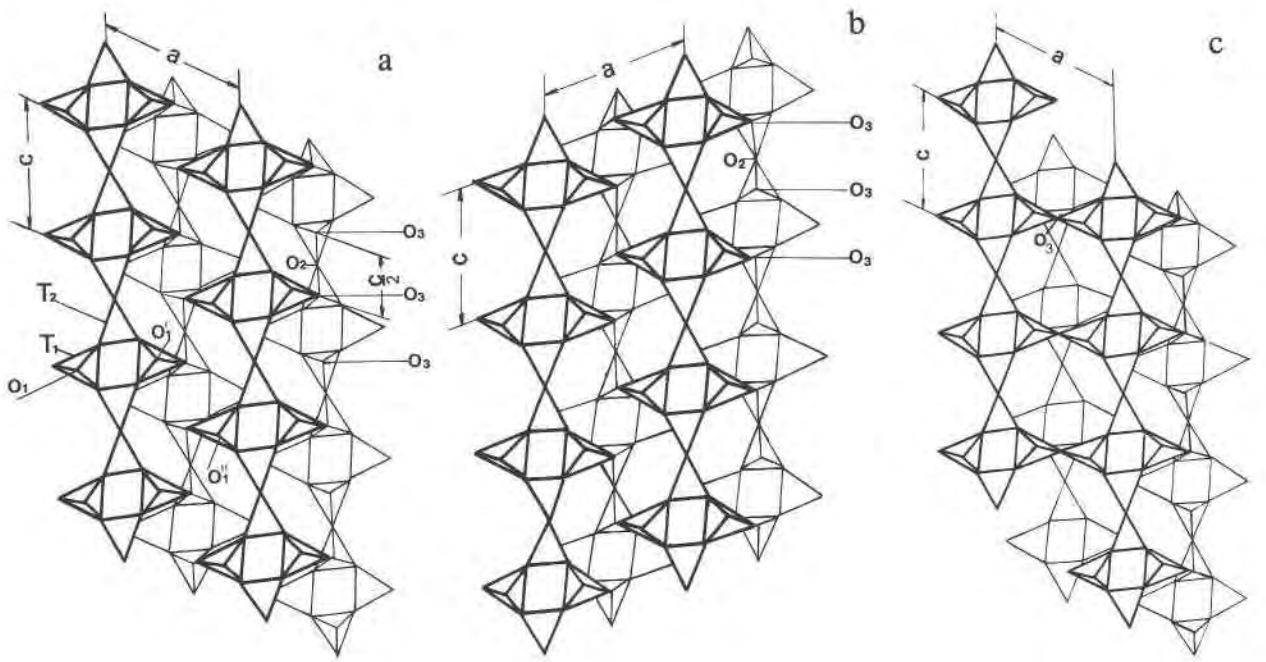

Fig. 2. Structure of feldspar. (**a**) Undistorted structure. Crankshaft chains of four-membered rings extend in the [100] direction. Straight chains extend in the [001] direction. Only the lower half of the thick-line ring is shown. The upper half is the reflection of the lower half in the mirror plane containing nodes O1, O1′, O1″. (**b**) Distorted structure. The faulting plane is parallel to (010) corresponding to Carlsbad twinning. Thin-line chains in the [001] direction are shifted by $c/2$. The lower part of the crystal is now in a twinning relation with the upper part. (**c**) Distorted structure. The faulting plane is parallel to (100). The right-hand portion of the crystal is shifted by **c**/2. The two parts of the crystal are connected by O3 nodes of thick-line chains extending in the [001] direction.

2a, then thin-line chains will be centered on this face with thick-line chains going through the corners.

There are two types of tetrahedra in each four-membered ring, T1 and T2. The nodes O1 of the T1 tetrahedra are situated on the (010) mirror plane and connect the two halves (upper and lower) of the thick ring. The nodes O2 of the T2 tetrahedra (Fig. 2a) are situated on the [010] twofold axis and connect two adjacent rings of the same chain.

Two prominent features in the unit-cell metrics and structure facilitate the probable layer shift by **c**/2:

1. Tetrahedral nodes common to two adjacent [001] chains (O3 in Fig. 2a) are situated near the line parallel to [001] and are separated by a distance close to $c/2$. For barium feldspar (Newnham and Megaw, 1960) with O2 at $x = z = 0$ and $y = 0.1382$, the coordinates of O3 are $x = 0.0262$, $y = 0.3101$, and $z = 0.2554$, and the separation of adjacent O3 is very close to $c/2$.

2. It follows from the cell dimensions that $a \cos \beta \approx c/2$.

The following models for stacking faults were considered:

Twinning by the Carlsbad law (Fig. 2b). Suppose that the centering (thin-line) [001] chains are shifted by **c**/2 (Fig. 2b). As a result of the sequence of O3 nodes separated by $\sim c/2$, this shift is easily accommodated in the feldspar structure by slight tilting of the T1 and T2 tetrahedra. From Figures 2a and 2b one can immediately recognize the two component parts of a Carlsbad twin (Bragg and Claringbull, 1965). These components are joined in the plane parallel to (010), which is the faulting plane in that model.

Coesite-like fault (Fig. 3a). If the upper half of the thick [001] chain is shifted by **c**/2 (Figs. 3a and 3b), we obtain the structural feature characteristic of the high-pressure silica polymorph coesite, in which the (010) mirror plane of feldspar is replaced by a *c*-glide plane. The relationship between these two structures has been discussed in detail by Megaw (1970). She showed that by a tilting of the T1 tetrahedra, the nodes O1′ of the upper half of the four-membered ring (Fig. 3a) are connected, after shifting by **c**/2, to the corresponding nodes of the lower part of the four-membered ring of the adjacent chain (O1″ in Fig. 2a). In this case condition $a \cos \beta \approx c/2$ is essential. The faulting plane is (010), as in model 1.

Faulting in the plane parallel to the (100) plane (Fig. 3c). We can divide the crystal into two parts along a plane parallel to (100) and shift the right part by **c**/2. Because $a \cos \beta \approx c/2$, the two parts may be sewn together. Two thick-line chains will then be directly connected by the nodes O3 (Figs. 3a and 3c). However, for this to happen, significant rearrangement of the tetrahedra of the centering (thin-line) chain must take place in order to satisfy this type of fault. For example, the O3 nodes facing up-

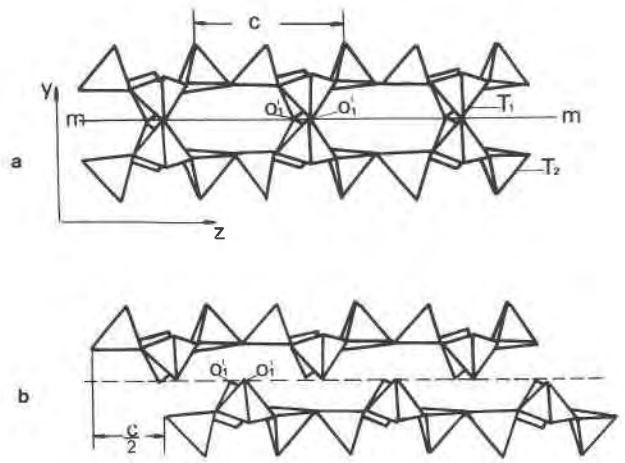

Fig. 3. Side view [in a direction normal to the (100) plane] of the thick [001]-extended chain. (**a**) Undistorted structure. Only the lower half of this chain is shown in Figure 2a (thick lines). (**b**) Coesite-like faulting. The lower half of the thick chain is shifted by **c**/2. After tilting of the tetrahedra, the nodes O1′ connect adjacent chains extending in the [100] direction.

ward (Fig. 2a) must be inverted downward in Figure 2c. It is, however, unlikely that such a configuration would occur, and this third type of fault is thus much less probable than the first two types described above.

Results

The theory for peak broadening for the type of stacking faults considered here has been presented by Wilson (1949). If the fault is represented by a shift of half of the cell by **c**/2, then reciprocal lattice points with l = even will be unchanged. The points with l = odd are extended in the direction of the **b*** or the **a*** reciprocal axis, depending on the actual faulting plane—(010) or (100). The reciprocal lattice for these two cases is shown schematically in Figure 4. Figure 4a applies to the first two models of stacking faults outlined in the previous section, and Figure 4b corresponds to the third model.

The distribution of the diffracted intensity (I) in the reciprocal space around the points with l = odd is easily derived from equation 5-24 given by Wilson (1949):

$$I = I_0/(1 + \pi^2 w^2/\alpha^2) \tag{1}$$

where α is the probability of the fault, w is the distance in reciprocal space along **b*** (Fig. 4a) or **a*** (Fig. 4b), and I_0 is the intensity at $w = 0$.

In the case of the (010) faulting plane and reciprocal lattice rods extending along **b***, w is defined as $w = k - k_0$, where k_0 is the index of the corresponding reciprocal lattice point and k is any positive real number, not necessarily an integer. In the case of the (100) faulting plane, $w = h - h_0$, with similar definitions of h_0 and h. The full width at half maximum of the diffraction peak expressed by Equation 1 is equal to

$$w = 2\alpha/\pi \tag{2}$$

where $w = \Delta k$ or $w = \Delta h$ for the (010) and (100) faulting planes, respectively.

Taking into account that the vector of any point in a reciprocal lattice $|S| = 2 \sin\theta/\lambda$, we can define the diffraction peak broadening through the variation of the reciprocal vector ΔS:

$$\Delta 2\theta = \Delta S\lambda/\cos\theta. \tag{3}$$

The value of ΔS can be derived from the general expression for S for a monoclinic lattice:

$$S^2 = \frac{1}{d^2} = \frac{h^2}{a^2\sin^2\beta} + \frac{k^2}{b^2} + \frac{l^2}{c^2\sin^2\beta} - \frac{2hl\cos\beta}{ac\sin^2\beta}. \tag{4}$$

The variables are k in the case of the (010) faulting plane and h in the case of the (100) faulting plane. Thus, taking into account expressions 1, 3, and 4, we arrive at the following expressions for peak broadening:

$$\Delta 2\theta = \frac{\lambda^2}{b^2}\frac{1}{\sin 2\theta}k_0\Delta k \tag{5}$$

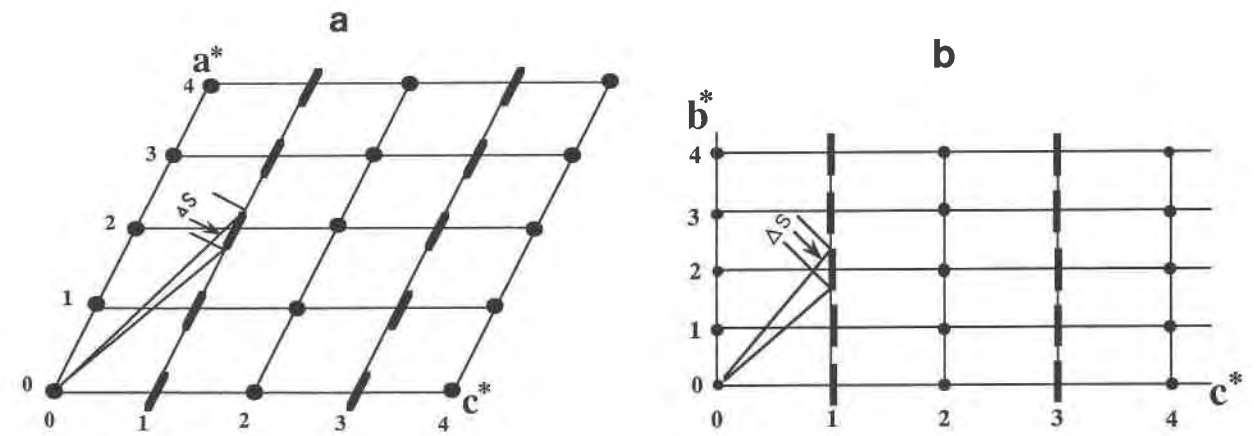

Fig. 4. Reciprocal lattice for distorted structures. (**a**) Faulting plane (010) and (**b**) faulting plane (100).

for the (010) faulting plane, and

$$\Delta 2\theta = \frac{\lambda^2}{a^2 \sin^2 \beta} \cdot \frac{1}{\sin 2\theta} (h_0 - l_0 \cos \beta) \Delta h \qquad (6)$$

for the (100) faulting plane, when l_0 is the reciprocal lattice point along **c***.

The $\Delta 2\theta$ values were calculated for various diffraction peaks with l = odd indices and compared with the observed data. Scaling of the calculated values was achieved by equalizing the mean experimental and calculated peak widths (Table 2).

Discussion

The observed peak widths for various peaks with l = odd are spread over a rather wide range—0.30° to 1.10°—and provide a sound basis for comparison of stacking fault models. These data correspond much more closely to the values calculated for the (010) faulting plane models (Table 2), the coefficient of correlation of observed and calculated data being 0.84 for the (010) vs. 0.30 for the (100) faulting plane model. This finding is not unexpected, since, as was noted earlier, the stacking fault in the (100) plane is accompanied by much greater structural distortion than stacking faults in the (010) plane (Figs. 2b, 2c, and 3b).

The probability of faulting may be estimated by Equations 2 and 5. Taking the experimental data for the sample annealed at 1050 °C (Table 2), the α value averaged over six measured peaks is equal to 0.1, emphasizing the high concentration of defects.

There are, however, two possible models for stacking faults in the (010) plane: Carlsbad twinning and the coesite-like model. Analysis of the lattice parameter trends gives us a clue as to which of the two models is more applicable. The appearance of defects is accompanied by a decrease in the lattice parameters (Table 1). This effect is particularly pronounced for parameter a, slightly greater than the estimated errors for c and β, and almost negligible for b. According to the analysis carried out by Megaw (1970), the imaginary feldspar-coesite transition must cause a decrease in the a and b parameters and an increase in the monoclinic angle β by several degrees. This predicted trend does not correspond with the observed variation of lattice parameters (Table 1), and thus the coesite-like fault model is not applicable. On the other hand, Carlsbad twinning should affect the a parameter to a greater extent than the other lattice parameters. Indeed, the nodes O3 that must overlap after shifting of the thin-line chains by **c**/2 are separated by $\Delta z = (0.2554 \times 2)c = 0.5108c$, where $z = 0.2554$ is the coordinate of the O3 atom. The difference of $0.0108c \approx 0.08$ Å must be accommodated by a decrease in the c parameter. The same nodes are separated in the x direction by $\Delta x = (0.0262 \times 2)a \approx 0.5$ Å, and greater decrease is likely for the lattice parameter a. Thus, the experimental data regarding the lattice parameters are better suited to the twinning model. In addition, this model apparently causes smaller structural distortion than the coesite-like model.

References cited

Belov, N.V. (1953) Crystal chemistry of feldspars. Proceedings of Lvov Mineralogical Society, N7, 10–20 (in Russian).

Bogdanova, G.S., Orlova, E.M., and Zevin, L.S. (1965) Phase composition of glass-ceramics in the system SiO_2-Al_2O_3-BaO-TiO_2. Bulletin of the Academy of Science, USSR, Inorganic materials, 1, 1816–1820.

Borg, I.Y., and Smith, D.K. (1969) Calculated powder patterns. Part II. Six potassium feldspars and barium feldspar. American Mineralogist, 54, 163–181.

Bragg, L., and Claringbull, G.F. (1965) Crystal structure of minerals, 288 p. G. Bell and Sons, London.

Megaw, H.D. (1970) Structural relationship between coesite and feldspar. Acta Crystallographica, B26, 261–265.

Newnham, R.E., and Megaw, H.D. (1960) The crystal structure of celsian (barium feldspar). Acta Crystallographica, 13, 303–312.

Smith, J.V. (1974) Feldspar minerals. Springer-Verlag, New York.

Wilson, A.J.C. (1949) X-ray optics. Methuen and Co., London.

Manuscript received July 17, 1990
Manuscript accepted August 28, 1991